Growing Single Crystals of High-Purity Refractory Metals by Electron-Beam Zone Melting

V.G. Glebovsky and V.N. Semenov

Institute of Solid State Physics, 142432 Chernogolovka, Russia

ABSTRACT

Crucible-less methods are very important and useful for melting, study and preparation of high-purity refractory metals and alloys because of the high melting points and chemical reactivity of these materials in the liquid state. The modified electron-beam floating zone melting (EBFZM) technique has been used for purification of refractory metals from both gaseous and metallic impurities and for growing single crystals. The growing processes of bicrystals of refractory metals from the melt, with desired grain boundary type and other bicrystalline parameters, have also been studied. Application of the EBFZM technique to the growth of W and Mo single crystal tubes is discussed, and the possibilities of using the EBFZM technique for preparation of highly pure refractory metals and alloys for advanced technologies are shown.

1. INTRODUCTION

Single crystals of high-purity refractory metals (Nb, Ta, Mo, W, etc.) are widely used in materials science and technology. This stimulates the study of the processes of purification and the development of new techniques for growing single crystals of well-defined crystallographic structure. A new version of the electron-beam floating zone melting (EBFZM) technique was developed in the Institute of Solid State Physics, Chernogolovka. It was used to prepare and study the macro- and microstructure of polycrystals, the substructure of single crystals and bicrystals of highly pure refractory metals, etc. The influence of the vacuum zone melting parameters such as growing rates, seed rotation rate, fluctuations of the electron-beam intensity, heat nonuniformities on the fronts of melting and solidification, influence of the seed substructure on the crystal perfection, etc., was studied. The specific features of the growth of polycrystalline and monocrystalline hollow cylinders were also studied.

We present a review of the EBFZM experiments on refractory metals, which are performed in the Institute of Solid State Physics, Chernogolovka. It will be shown that this technique is very useful both for the preparation of metals with low gaseous interstitial impurity content, and for the growth of single crystals with desired crystallographic parameters.

2. ELECTRON-BEAM ZONE FURNACE

The EBFZM furnace (Fig. 1) consisted of a vacuum-melting chamber, a device for crystal rotation, a device for vertical displacement of an electron-beam gun, a vacuum pump system and an electric supply /1,2/. The water-cooled stainless-steel vacuum chamber was made of two vertical parts. The upper part can be moved vertically and provided easy adjustment of the specimens and the electron-beam gun. The most important part of the furnace was the electron-beam gun (Figs. 2 and 3), which consisted of a circular cathode and the set of water-cooled Cu focusing electrodes.

Fig. 1: Electron-beam floating zone melting furnace for purification refractory metals and for growing single crystals.

The melting specimen served as an anode for the electron-beam gun and therefore was part of the electrical circuit, together with the electron-beam gun W filament at a current of 40 A and a potential, between the cathode (the W filament) and the anode (the specimen), of +20 kV. Depending on the arrangement of focusing electrodes, the electron beam could be varied from a diffuse type to a sharp one, as shown in Fig. 4. The continuous lifetime of the electron-beam gun at melting procedures was practically unlimited and, in principle, depended only on the lifetime of the W filament. As a rule, the filament lifetime was about 100 hours.

The crystal-rotation rate was 60 rpm, which was enough for the thermal and compositional homogenization of the liquid zone. Depending on the procedure, the melting rate (or the electron-beam gun travelling rate) varied from 0.5 to 50 mm min^{-1}; however, the regular melting/growing rate was about 2 mm min^{-1}. The new version of the EBFZM technique gave the possibility of growing polycrystalline and monocrystalline rods of 4 – 30 mm in diameter and 50 – 600 mm in length for practically all refractory metals studied. Growing long single crystals (up to 1100 mm)

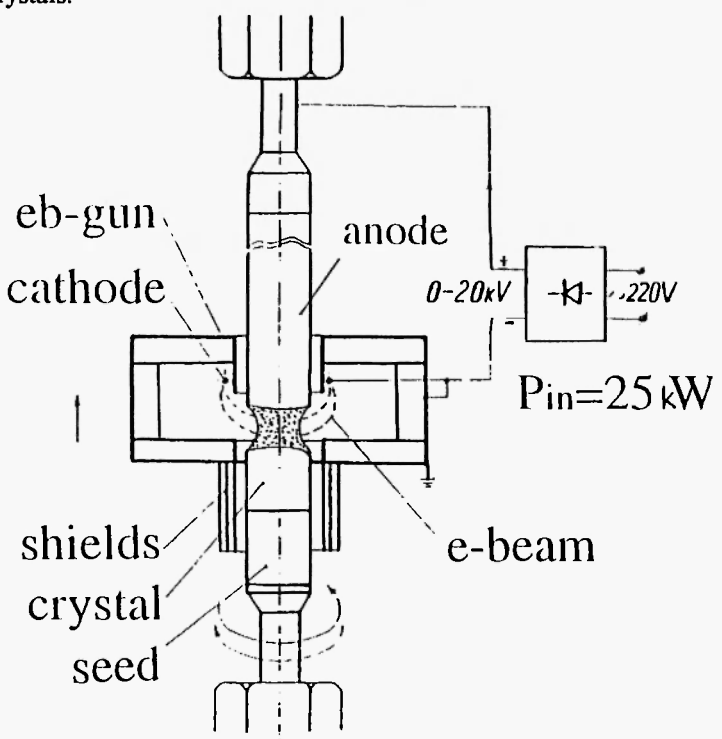

Fig. 2: Schematic diagram of crystal growth by EZFZM.

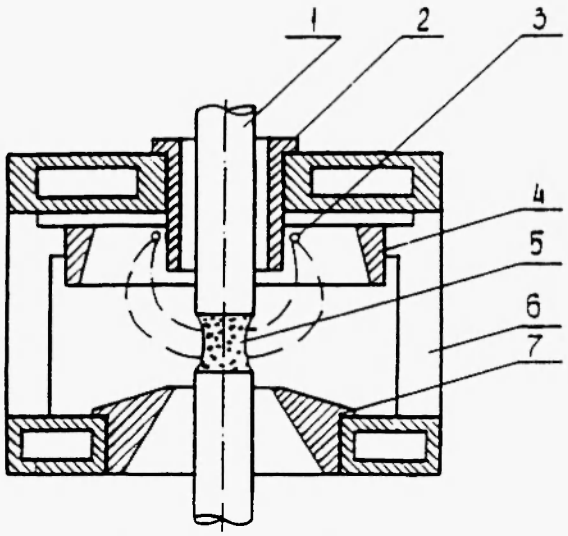

Fig. 3: Schematic diagram of circular electron-beam gun for crystal growth by EBFZM. *1* - melting/solidifying cylindrical specimen, *2, 4* and *7* – water-cooled Cu focusing electrode, *3* – circular cathode (W filament), *5* – zone of liquid metal, *6* - water-cooled Cu massive body.

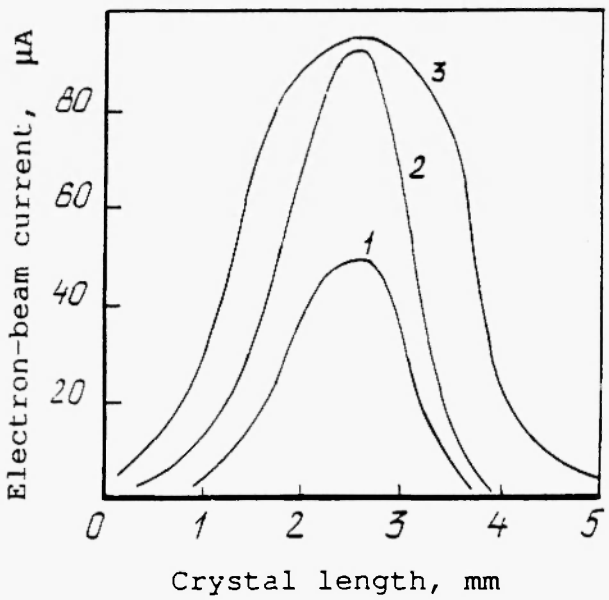

Fig. 4: Electron-beam focusing patterns (electron-beam current vs. crystal length). *1* and *3* – diffuse electron beam, *2* – sharp electron beam.

on the monocrystalline seeds was also possible, and it was shown that the growth axes of the single crystals and the orientations of the monocrystalline seeds used coincided with an accuracy of 2°. We take this to be evidence of the excellent performance of the electron-beam gun and the mechanical devices for gun travel and specimen rotation.

3. PURIFICATION OF REFRACTORY METALS

An important advantage of the floating zone vacuum technique is the possibility of purification of liquid metals by the removal of gases in vacuum. Likewise, volatile impurities can be vaporized. The purification process of the refractory metals (Nb, W, Mo, Ta, V, Ti) from metal and gaseous impurities were studied, as well as some electrophysical properties (e.g. specific electric resistivity) /3/. The data on the typical chemical composition of Mo, W and Nb are presented in Table 1.

The results of our experimental study of the removal of O and C impurities from the liquid Nb seem to be of interest and therefore will be discussed in more detail. Niobium is a typical refractory metal with high chemical activity and has been studied very intensively in recent years. Nevertheless, many features of vacuum purification of liquid Nb from gaseous impurities are not clear yet /4/. At the same time, it is well known that the microstructure and physical properties of Nb are mainly dependent on its purity and structure. Therefore the interstitial content in Nb, mainly O and C, is of interest in high-purity Nb single crystals. There are two main processes determining the final O and C content in the Nb: (a) desorption of Nb monoxide, NbO, and (b) desorption of C monoxide, CO. During these two competitive processes, the situation arises when the removal of C is nearly stopped at a certain O content /5/. Empirical attempts to understand the reason for this behaviour of C in refractory metals, and to find ways that allow the lowering of the C content in the Nb by a combination of oxidation and high-vacuum annealing, were not wholly successful. From our point of view, the absence of reliable high-sensitivity methods and quantitative physicochemical data on the behaviour of O and C in Nb during vacuum melting

Table 1
Chemical composition of refractory metals (ppm).

	Mo	W	Nb		Mo	W	Nb
O	<0.5	<0.5	<0.1	Mn	<0.03	<0.3	<0.03
C	<0.5	<1.0	<10	Nb	<0.3	<0.1	<0.3
N	<0.6	<0.6	<0.6	Ta	<0.1	<0.1	<50
H	<1.0	<1.0	<1.0	Re	<0.1	<0.1	<0.1
Si	<0.3	<0.3	<0.3	V	<0.03	<0.3	<0.03
Al	<0.1	<0.1	<0.1	Fe	<0.03	<0.1	<0.03
K	<0.1	<0.1	<0.1	Ni	<0.03	<0.06	<0.03
Ca	<0.1	<0.1	<0.1	Co	<0.3	<0.3	<0.3
Na	<0.01	<0.3	<0.01	Cr	<0.03	<0.05	<0.03
P	<0.03	<0.3	<0.03	Cu	<0.03	<0.05	<0.03
S	<0.1	<0.3	<0.1	Pb	<0.1	<0.1	<0.1

and annealing are mostly responsible for the situation.

A study of the O/C transport and the removal kinetics in the process of electron-beam zone vacuum purification of Nb was performed using fast-neutron activation analysis /4,5/. The analysis was non-destructive and used an on-line neutron activation detector with an analytic sensitivity of 10^{-5} %. The energy of the fast neutrons was about 14 MeV. The principal advantage of the detector was the *in-situ* fast automatic cleaning of the specimen surface by strong etching for 5-7 s, which was extremely important for the short-life isotope analysis. The C content was determined by two methods, by burning a sample in an oxygen flow, the detection limit being 10^{-3} %, and by deuteron activation, the detection limit being 10^{-6} %.

Two types of starting Nb rods were used. To study the O removal, C-free Nb rods were prepared with an O content of about 10^{-2} %. To study the O/C interaction and the removal of both O and C, O/C doped Nb rods of 20 mm in diameter and 200 mm in length were prepared by powder metallurgy techniques /5/. The O content in the starting material was (3 - 16) x 10^{2} %, the C content was (15 - 80) x 10^{-3} % and the O/C ratio was 2. The travelling rate of the crystallization front was 2 mm min^{-1}. The number of zone-remelting passes in vacuum was from 1 to 30. As our experiments showed, the O and C were homogeneously distributed in the zone-purified crystals. To show the dependence of the O content in Nb on the zone numbers, as well as the influence of surface contamination of the Nb specimens on the experimental results, 23 Nb single crystals were zone-purified in vacuum with the liquid-zone pass numbers varying from 1 to 30.

Several procedures for surface cleaning (*in-situ* strong etching, without etching, preliminary chemical polishing) were used as well. It was found (Fig. 5) that the O content, determined by vacuum-extraction analysis (with or without etching and preliminary chemical polishing), corresponded to the fast neutron activation analysis data (without *in-situ* etching) for the same specimens. The O content, determined by activation analysis of *in-situ* etched specimens (< 1 x 10^{-5} %), was much lower than for the same samples without *in-situ* etching (5 x 10^{-2} %). It was also found that during the first liquid-zone pass in vacuum, the O extraction rate was much higher than during subsequent passes. The study of the O behaviour during multiple liquid-zone melting in vacuum demonstrated that the O transport from the bulk to the liquid metal-vacuum interface was much slower than O desorption from the liquid-zone surface into vacuum. The experimental results also demonstrated that the

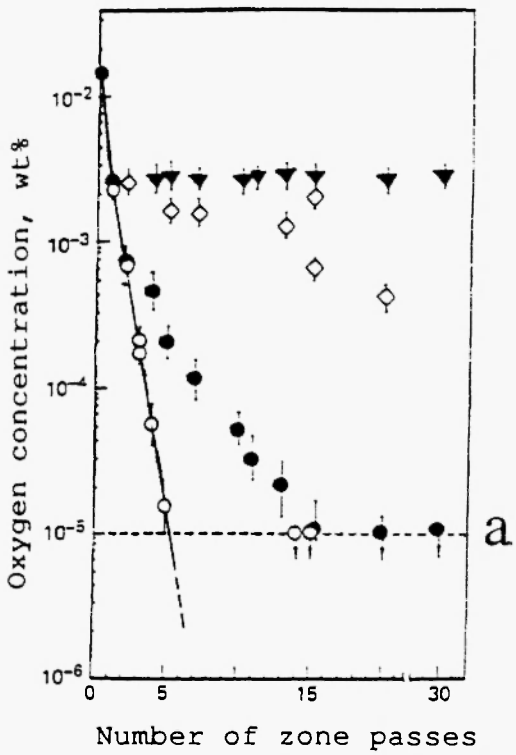

Fig. 5: Oxygen content in the Nb single crystals vs. numbers of liquid zone passes in vacuum
a – detecting limit of fast neutron activation with *in-situ* strong etching, • and o – oxygen content in Nb after different vacuum zone-melting procedures, ▼ - fast neutron activation without *in-situ* etching, ◊ - oxygen content analysed by vacuum-extraction melting.

mechanism of O desorption did not change in a wide range of the O concentrations from 10^{-2} to 10^{-5} %. The conclusion reached was that former observations of the change of the O desorption mechanism during purification of refractory metals was conditioned by the low sensitivity of analytical methods used, as well as by the inadequate surface cleaning of the specimens.

The results of the study of the O/C interaction in the O/C-doped Nb specimens showed that the effectiveness of C removal did not depend on the O/C ratio in the starting Nb specimens but depended only on the difference between the initial O content and a critical value. It appeared that the greater this difference, the lower the resultant C content. It was shown that there existed a certain critical O content which, when attained, slowed down the rate of C removal drastically and the C content tended toward an ultimate value. The most important result of the studies /4,5/ was the following: the lowest content of both O and C (< 10^{-5} %) was obtained using the multiple electron-beam floating zone melting in a vacuum of less than 10^{-6} torr.

4. GROWING SINGLE CRYSTALS

The dislocation structure of refractory metal single crystals (Nb, Mo, W) showed a considerable similarity and varied only slightly within the range of the crystal growing rate from 0.5 to 5 mm min^{-1} /6/. A typical substructure of W single crystal is shown in Fig. 6. The longitudinal cross-sections exhibited subgrains elongated along the growth axis, the normal cross-sections exhibited equiaxial subgrains, but there was a significant radial inhomogeneity of the substructure. The peripheral subgrains were more refined than the central ones. A noticeable change of the substructure occurred for increasing crystallization rates up to 10 mm min^{-1}. It involved the appearance of subgrains with a misorientation angle of up to 5°.

A typical subgrain size distribution in highly pure W single crystals is shown in Fig. 7. The mean subgrain size was 400 μm. The experimental dependence on the crystallization rate of the dislocation density in subgrains showed that at higher rates the

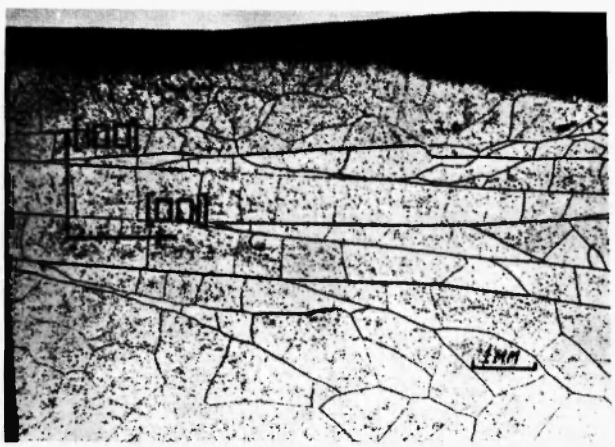

Fig. 6: Typical substructure of W <100> single crystal grown at a rate of 2 mm min^{-1} (longitudinal cross-section).

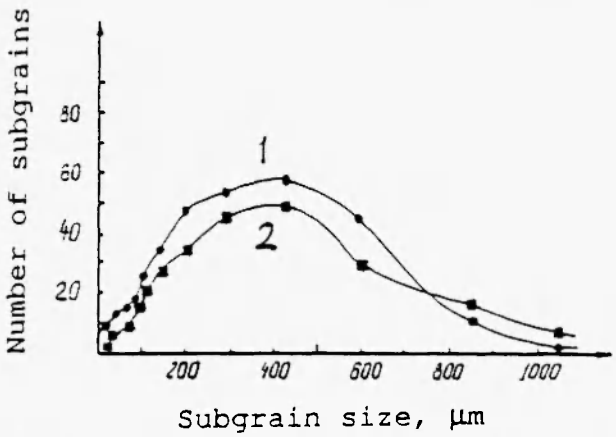

Fig. 7: Subgrain size distribution, *a* - along growth axis, *b* - normal to growth axis.

dislocation density increased by about an order of magnitude.

During the growing procedure of single crystals from the melt, the dislocations in the single crystals might arise as a result of (a) following the seed structure, (b) thermal stresses in the solid phase, (c) impurity content gradients, (d) lattice oversaturation with vacancies. An attempt was made to grow the W and Mo single crystals with a relatively perfect substructure using a monocrystalline seed, free from small-angle boundaries (Fig. 8). Such a seed was prepared by the strain-anneal technique. The density of dislocations in the seed was 10^4 cm^{-2}. It could be expected that a single crystal with perfect crystallographic structure would be grown, but it appeared that the subgrains penetrated from the seed into the single crystal, the dislocations arose inevitably again during growth, and the misorientation angle between subgrains gradually increased (Fig. 8). The X-ray topography patterns display the difference between the single crystal grown from the melt and that obtained by strain-anneal technique (Fig. 9).

Inasmuch as the residual resistivity ratio was about 10^4, the gaseous and metal impurities did not play an important role in the substructure formation. Probably the high thermal stresses were responsible for the substructure of the EBFZM-grown single crystals of highly pure refractory metals. The EBFZM is characterized by the presence of high axial temperature gradients in both the solid phase and the melt. According to our calculations of the gradients, on solving a one-

Fig. 8: Microstructure of W single crystal grown on the perfect monocrystalline seed. *a* – seed, *b* – grown single crystal.

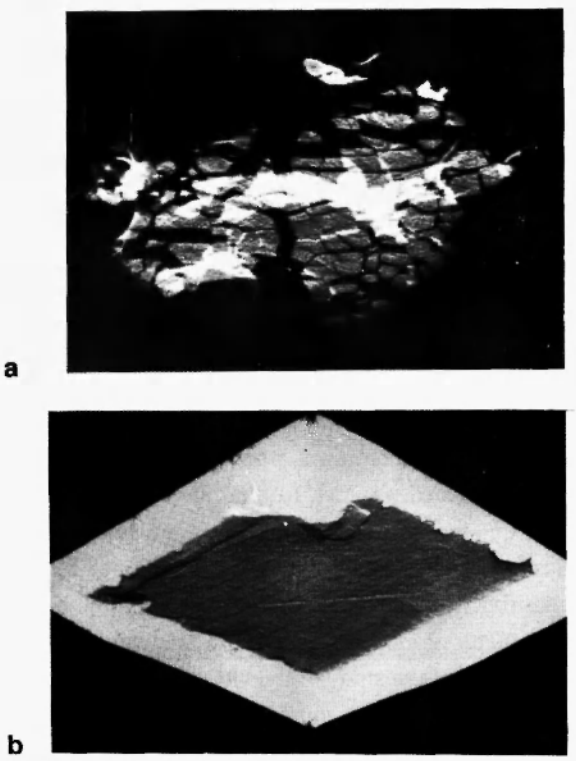

Fig. 9: X-ray angular scanning topography patterns. *a* – single crystal grown from the melt, *b* – single crystal prepared by strain-anneal technique.

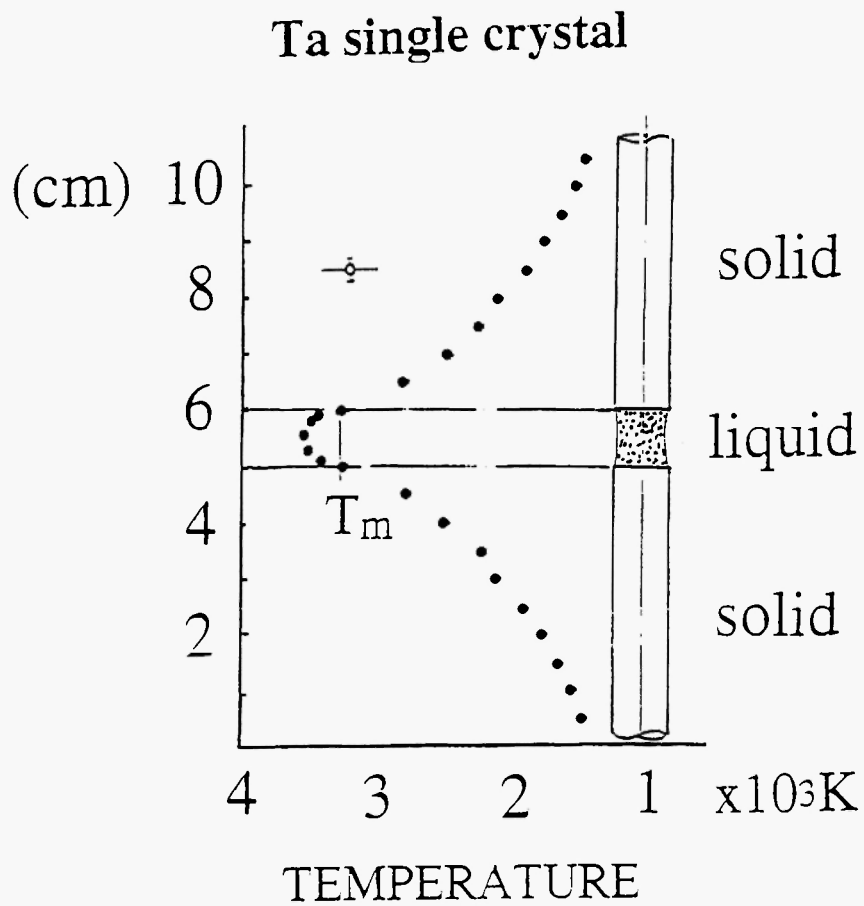

Fig. 10: Temperature distribution along the growth axis of Ta single crystal.

dimensional equation for thermal conductivity, and according to our measurements by micropyrometry (Fig. 10), the axial temperature gradients near the crystallization interface in Ta and W single crystals reached 1500 K cm^{-1}. At such high temperature gradients, high thermal stresses can arise. These could only be removed by dislocation motion. As a result, the axial temperature gradient appears to be responsible for the density of the non-removable dislocations. The calculations of the dislocation density, which was a result of the high axial temperature gradients, coincided with the measured dislocation density in the single crystals studied with a high degree of accuracy.

5. GROWING BICRYSTALS

To study physical properties of the large-angle grain boundaries, a technique for growing refractory metal bicrystals was developed. Using the modified EBFZM technique, bicrystals with a wide range of boundary planes and of misorientation angles were grown /7/. As-grown bicrystals of Nb, Mo and W were 25 mm in diameter and 150 mm long (Fig. 11). Figure 12 shows schematic diagrams of three methods used to prepare the bicrystalline seeds.

Molybdenum bicrystals with several different crystallographic indices of the boundary planes were tested for strength using three-point bending /8/. It was established that the large-angle boundaries in Mo bicrystals had a considerably lower strength compared with that of the small-angle boundaries. The majority of the bicrystalline samples had brittle fractures along grain boundaries; some of the samples tested had small areas of plastic deformation. Near the special tilt and twist boundaries, a characteristic strength minimum was observed. Studies of the fractured surfaces, carried out by optical microscopy and Auger-electron

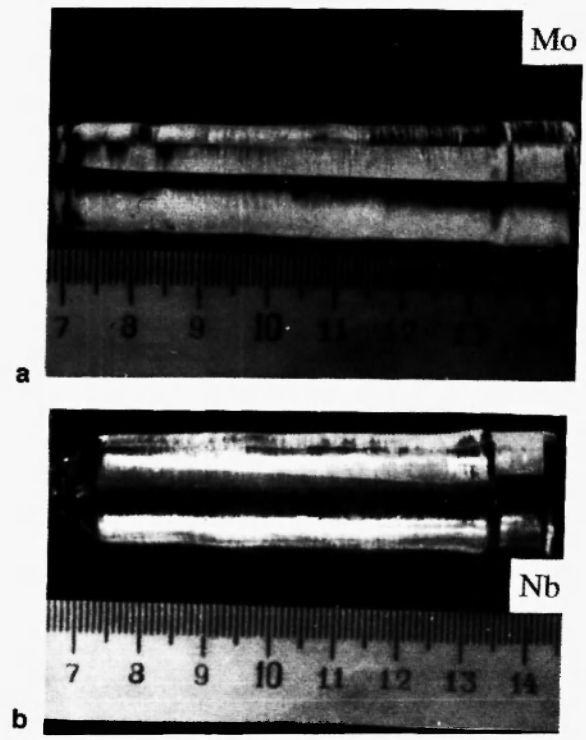

Fig. 11: Bicrystals of Mo and Nb. Slightly curved bicrystalline boundaries are seen on the surface of both bicrystals. *a* – molybdenum, *b* – niobium.

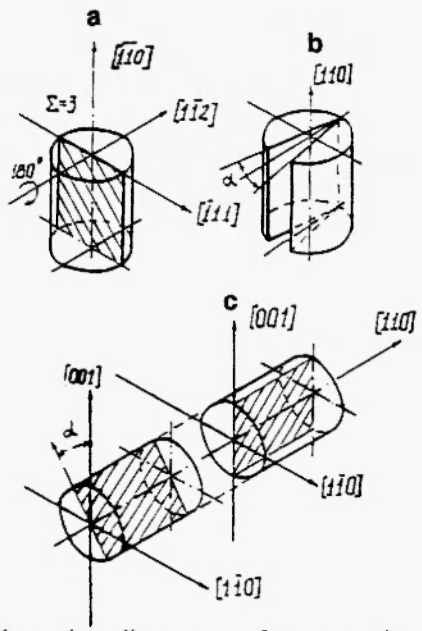

Fig. 12: Schematic diagrams of preparation of bicrystalline seeds. Choice of diagrams *a*, *b* and *c* depends on desired crystallographic parameters of the boundary.

spectroscopy, showed the presence of small second phase particles on the grain boundaries. The Auger-electron spectroscopy studies of the fractured surfaces revealed interstitial impurities, with their concentrations on the boundaries being one order greater than that in the grains. The studies of the boundary strength also showed that the large-angle grain-boundary strength mainly depended on the boundary type and the misorientation angle.

6. GROWING TUBULAR SINGLE CRYSTALS

Usually the refractory metal single crystals, grown by EBFZM, are rods. For new applications, it is of interest to grow hollow cylinders or tubes. It seems that the modified EBFZM technique, using the electron gun of high efficiency and of electron-beam uniformity, is the only method capable of growing tubular ingots of highly-pure refractory metals from the melt /8/. The stationary stage of the growing tube from the melt is shown schematically in Fig. 13. After vacuum degassing, a molten meniscus *2* was formed on the starting CVD-tube *1* and zone melting was used to grow tubular single crystals *3* of 200 mm in length. Since the walls of the tube were thin (about 1 mm), it was possible to ignore the gravitational forces acting upon the meniscus, and the size relationship between

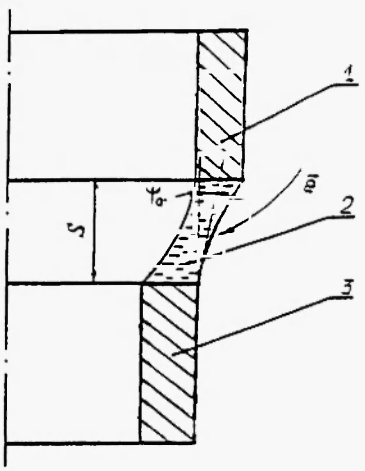

Fig. 13: Schematic diagram of growing monocrystalline tubes. *1* – starting tube, *2* – meniscus of molten metal (liquid zone), *3* – grown monocrystalline or polycrystalline tube.

the starting tube and grown crystal could be calculated by solving the Laplace equation in the thin-film approximation.

The metallographic studies of the dislocation structure of polycrystalline tubes, grown without seeds, showed that the tubes had many large-angle boundaries which were situated in the planes parallel to the growth axis (Fig. 14). The small-angle boundaries in monocrystalline tubes, grown on the seeds, were situated similarly (Fig. 15). The X-ray angular scanning studies of the normal cross-sections of the monocrystalline tubes (growth axis <111>, reflection (110)) showed that the misorientation angles between subgrains did not exceed 2° (Fig. 16). It was also of interest that the structure of single crystal rods and that of single crystal tubes was similar.

Fig. 14: Micrograph of large-angle grain boundary in W polycrystalline tube.

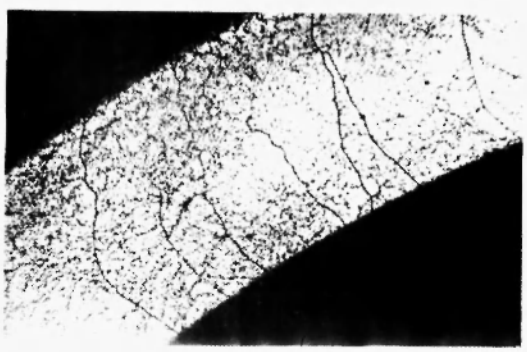

Fig. 15: Micrograph of small-angle grain boundaries in W monocrystalline tube.

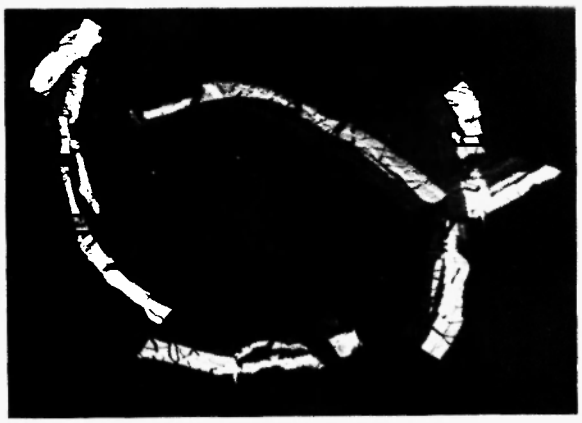

Fig. 16: X-ray angular scanning topography pattern of W monocrystalline tube.

7. CONCLUSIONS

The modified vacuum electron-beam floating zone technique is extremely useful for both purifying and growing single crystals of refractory metals because of the non-crucible nature of the technique. Both polycrystalline and monocrystalline rods, 4 - 30 mm in diameter and 50 - 600 mm in length, of all refractory metals can be produced. The growth axes of single crystals (600 - 1000 mm long) grown by the new version of the EBFZM technique coincide with the orientations of the single crystal seeds used. The dislocation structure of refractory metal single crystals grown by EBFZM depends on both the temperature gradient and growth rate. The substructure of single crystals is characterized by a relatively strong radial nonuniformity. Tubular single crystals grown by the EBFZM technique have a substructure similar to that of the cylindrical single crystals.

ACKNOWLEDGEMENTS

The authors are very thankful to Mr. Victor V. Lomeyko for providing the EBFZM experiments and to Prof. Dr. Hidde H. Brongersma for very interesting discussions. The studies were supported in part by the Russian Academy of Sciences and the Netherlands' Organisation for the Advancement of Scientific Research (NWO).

REFERENCES

1. V.G. Glebovsky and V.N. Semenov, in: *Proc. 13th Int. Plansee Seminar*, H. Bildstein and R. Eck (eds.), Metallwerk Plansee, Reutte/Tirol, Austria, **1**, 190 (1993).
2. V.G. Glebovsky, V.N. Semenov and V.V. Lomeyko, *J. Less-Common Metals*, **117**, 385 (1986).
3. V.G. Glebovsky, in: *Proc. 1st Int. Conf. on Refractory Metals*, Kitakoyushi, Japan, 1990, p. 191.
4. V.G. Glebovsky, I.V. Kapchenko and B.M Shipilevsky, *J. Alloys and Compounds*, **184**, 305 (1992).
5. V.G. Glebovsky and B.M. Shipilevsky, *J. Crystal Growth*, **60**, 363 (1982).
6. V.G. Glebovsky, V.N. Semenov and V.V. Lomeyko, *J. Crystal Growth*, **87**, 142 (1988).
7. V.G. Sursaeva, V.G. Glebovsky, Yu. M. Shulga and L.S. Shvindlerman, *Scripta Metall.*, 19, 411 (1985).
8. V.G. Glebovsky, V.N. Semenov and V.V. Lomeyko, *Vacuum*, **41**, 2165 (1990).